X-ray interference topography investigation of Si/Ge$_x$Si$_{1-x}$/Si(001) heterosystem

A A Fedorov, E M Trukhanov, A P Vasilenko, A V Kolesnikov and M A Revenko

Institute of Semiconductors Physics, 630090 Novosibirsk, Prosp. Lavrentyeva 13, Russia

E-mail: trukh@isp.nsc.ru

Abstract
In x-ray topographs of Si/Ge$_x$Si$_{1-x}$/Si(001) heterosystems, the intensity variations, which are associated with inhomogeneous GeSi thickness, are observed. The layers of GeSi and Si were grown by molecular beam epitaxy. The growth conditions preserving the pseudomorphic state of the intermediate SiGe layer from misfit dislocation appearance were kept. The topographs were recorded using a spherically bent monochromator as well as a flat one. The observed contrast peculiarities are established to be Moiré (translation fault) fringes. The displacement of interference fringes due to the crystal angular position variation is observed. For Pendellösung maxima, the dependence of their angular positions on nondiffracted layer thickness is established. The image simulated in the framework of semikinematical approach demonstrates the main contrast peculiarities observed in the topograph.

1. Introduction

Three-layer heterosystems of *A*/*B*/*A*, where *A* and *B* are different crystals, are widely used for x-ray diffraction investigations [1–8]. The heterosystem parameters are often determined by the rocking curve simulation and the following comparison of results with experimental data. Any dependence between the angular peak position and the thickness of an intermediate layer *B* has not been discussed in the literature [3, 9, 10]. In x-ray topographs of *A*/*B*/*A* heterosystems obtained at the rocking curve maximum, significant intensity variations down to zero are observed [11–14]. The authors [11] described these contrast variations as Moiré fringes which appeared due to slightly distorted lattice of the upper crystal A. In papers [12, 15] these fringes were described as translation fault fringes. It should be mentioned that in [16] these translation fault fringes were considered as a variant of Moiré fringes (dilatational and/or rotational ones) appearing in an inhomogeneous deformed bicrystal. This paper is aimed at the investigation of the Si/GeSi/Si heterosystem with layers, which were not damaged during preparation in contrast to systems used in [11–13, 17, 18].

2. Experimental

Two Si/Ge$_x$Si$_{1-x}$/Si(001) heterosystems with $x = 0.09$ and $x = 0.2$ were grown by molecular beam epitaxy. As the Ge$_x$Si$_{1-x}$ layer was growing, the wafer was partly shielded by a mobile screen in order to provide variation in the thickness of the separating Ge$_x$Si$_{1-x}$ layer from some maximum value to zero. The obtained structures are shown schematically in figures 1(*a*) and 2(*a*). The layer thickness t changed in steps (figure 1(*a*)) or with an approximately constant gradient (figure 2(*a*)). The maximum layer thicknesses (t_{max}) were chosen to preserve the pseudomorphic state of the intermediate solid solution layer from misfit dislocation appearance: $t_{max} = 40$ nm for $x = 0.2$, and $t_{max} = 90$ nm for $x = 0.09$. The upper silicon film with the thickness of t_{Si} =1 μm was grown over the solid solution layer. Diffraction and topography investigations were carried out in $(n, -n)$ nondispersive Bragg geometry using CuK$_{\alpha1}$ radiation and reflections 004, 113 and 224 (the asymmetry factor is $b = 0.06$ and 0.16 for (113) and (224) reflections, respectively). For the topography investigations with the spherical incident wave, a monochromator of (225) orientation providing a convergent
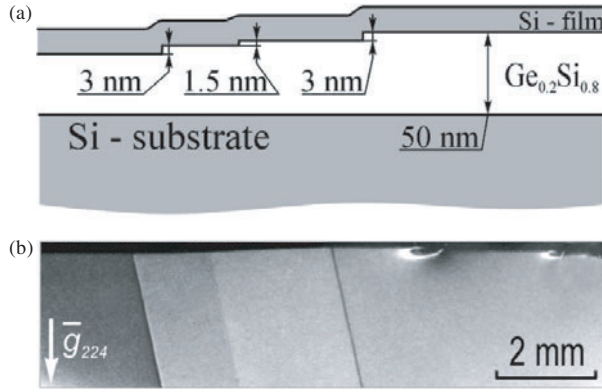
Figure 1. Scheme of the investigated part of the Si/Ge$_{0.2}$Si$_{0.8}$/Si(001) heterosystem (*a*) and interference images of the steps in the topograph (*b*).
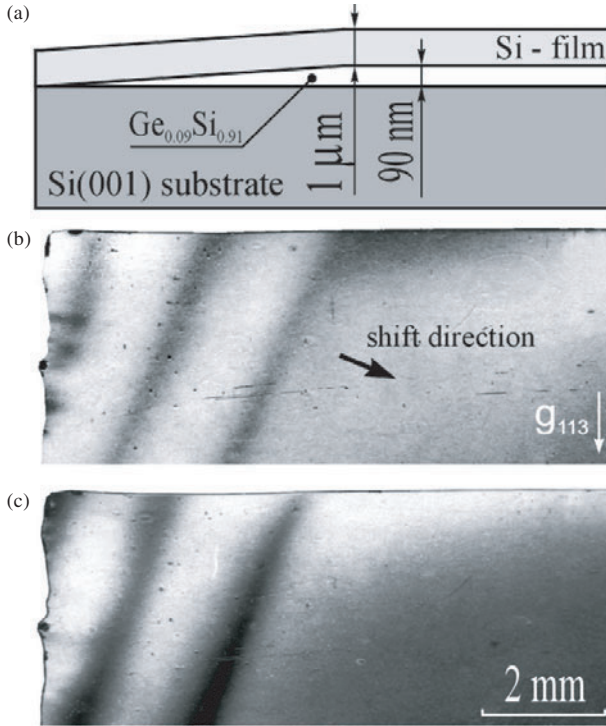
Figure 2. Scheme of the Si/Ge$_{0.09}$Si$_{0.91}$/Si(001) heterosystem (*a*) and displacement of the interference fringes due to the difference (12 arcsec) between sample angular positions used in getting the topographs (*b*) and (*c*).

Figure 3. Topograph of the heterosystem (figure 2(*a*)) obtained using a spherically bent monochromator (*a*) and the corresponding simulated image (*b*). The interference effects indicated with lines A–D are observed for the wedge region of the Ge$_{0.09}$Si$_{0.91}$ separator.

outlet beam was used. It presented a 400 μm thick Si wafer, which is elastically curved with curvature radius of about 6 m. The topograph (figure 3(*a*)) was recorded using a spherically bent monochromator, and the topographs (figures 1(*b*), 2(*b*) and (*c*)) were recorded using a flat one.

3. Results

The principal features of the topograph (figure 1(*b*)) are the intensity variations associated with the GeSi layer steps. No variations are observed in topographs obtained from the heterosystem areas with the fixed thickness of the intermediate layer. It can mean that the crystal lattice parameters of Si film and substrate are the same, and any distortions of film crystal lattice are absent. But this is not a highly probable case. Another case means that the ΔH vector, which is the difference between the reciprocal-lattice vectors H of the film and substrate, is perpendicular to the sample surface [17, 19]. It means that the film lattice is tetragonally distorted.

The theory of Moiré pictures in a bicrystal with a nondiffracted layer is presented in [20]. For ΔH perpendicular to the sample surface, the intensity of the diffracted wave can be written in the Bragg case as:

$$I_H(\mathbf{r}_s) = \left| \frac{[\rho_{HA}\tau_{HB} + \tau_{0A}\rho_{HB}\exp(2\pi i\Phi)]}{[\tau_{HA}\tau_{HB} + \rho_{0A}\tau_{HB}\exp(2\pi i\Phi)]} \right|^2,$$

where τ_0 and τ_H are the transmission coefficients along the forward-diffracted and diffracted directions, respectively; ρ_0 and ρ_H are the reflection coefficients in these two directions, respectively, A and B are the symbols for the first (entrance) and second crystals. The phase can be written as $\Phi = \Phi_{\text{Moiré}} + \Phi_{\text{gap}} + \Phi_{\text{refr}} + \Phi_{\Delta H,\text{Bragg}}$, where $\Phi_{\text{Moiré}} = \Delta H \mathbf{r}_s$, $\Phi_{\text{gap}} = -\eta t/\Lambda_0$, $\Phi_{\text{refr}} = kt\Delta\chi\Delta\gamma/2$ and $\Phi_{\Delta H,\text{Bragg}} = (t_1 + t)\Delta H(s_H/\gamma_H + s_0/\gamma_0)/2$. Here $\mathbf{r}_s$ is any position on the entrance surface, Λ_0 is the Pendellösung length, η is the normalized angular coordinate, t_{Si} and t are the thicknesses of the first crystal and the gap, respectively, $k = 1/\lambda$ is the vacuum wavenumber, $\Delta\chi = \chi_0 - \chi_{0,g}$ is the difference of the refractive indices between the gap and the crystal, $\gamma_0 = n s_0$ and $\gamma_H = n s_H$, n is the surface normal, s_0 and s_H are the unit vectors in the forward-diffracted and diffracted directions, respectively, $\Delta\gamma = 1/\gamma_H - 1/\gamma_0$.

Since the ΔH vector is perpendicular to the sample surface, then $\Phi_{\text{Moiré}} = 0$. For other parts of Φ let us consider their variations with 3 nm changing of t_{gap}. For the reflection 224 and $|\eta| \leqslant 10$, the maximum values of their variations are $\Delta\Phi_{\Delta H,\text{Bragg}} \leqslant 3 \times 10^{-3}$, $\Delta\Phi_{\text{refr}} \leqslant 2 \times 10^{-3}$ and $\Delta\Phi_{\text{gap}} < 10^{-2}$. Thus, the intensity variation up to 0.2 (see the left step of 3 nm high in figure 1(*b*)) cannot be explained in the framework of the models [20]. Note that the observed contrast peculiarities are fundamentally different from those

investigated in [21, 22], since the thickness of the intermediate layer is far less than Λ_0.

Intensity variations presented in figure 1(*b*) and associated with the GeSi layer steps do not arise from inhomogeneous lattice parameter distribution in the upper crystal, similar to those observed in [13] and analysed in [23] using Takagi–Taupin equations, since crystal lattice parameter of the used epitaxial film was constant through the thickness.

The mentioned intensity variations can be explained in the framework of the models [15, 16]. In both concepts, the intensity distribution is periodic because it includes the term $\sin(2\pi \mathbf{H} \cdot \mathbf{u})$ [15] or $\cos(2\pi \mathbf{H} \cdot \mathbf{u})$ [16], where $\mathbf{u}$ is displacement of the atoms in the upper crystal relative to those in the substrate. If the inhomogeneous variation of $\mathbf{H} \cdot \mathbf{u}$ ranges up the integer m, then m interference fringes appear. In our previous paper [24], it is shown that if $\mathbf{u}$ is perpendicular to the crystal surface, then condition $\mathbf{H} \cdot \mathbf{u} = m$ results in displacement of the corresponding planes in the upper film and substrate at the value of md_{hkl}. Thus, the $|\mathbf{u}_0|$ value, which is necessary for appearance of an additional fringe, is $|\mathbf{u}_0| = d_{hkl} / \cos \varphi$, where φ is the angle between the (*hkl*) plane and the sample surface.

To obtain the dependence between $\mathbf{u}$ and GeSi thickness variation, let us consider the difference δa between the substrate and film lattice parameters taken along the growth direction. For the pseudomorphic state of GeSi, this value is $\delta a = \Delta a (1+\nu)/(1-\nu)$, where ν is the Poisson coefficient and Δa is the mentioned difference between parameters in the case of a nonstressed GeSi layer. An increase of the separating layer thickness by $N(a + \delta a)$ results in $|\mathbf{u}| = N\delta a$, where N is the integer. Its minimum value, which is necessary for appearance of an additional interference fringe, is $N_{\min} = d_{hkl}/(\delta a \cos \varphi)$. The corresponding thickness variation of the GeSi layer is

$$t_{\min} = N_{\min}(a + \delta a) \approx \frac{a d_{hkl}}{\delta a \cos \varphi} = \frac{a}{\delta a} \frac{d_{hkl}}{\cos \varphi} = \frac{a}{\delta a} |\mathbf{u}_0|.$$

A similar expression is given in [5] to describe interference effects in a three-layer system in terms of kinematical approach. Taking $\nu = 0.28$ for $Ge_{0.2}Si_{0.8}$, one gets $t_{\min} = 8.87$ nm for 224 reflection. Thus, the t_{gap} change of 3 nm causes the phase term change of 0.3 and the intensity variation up to 30%, which is in agreement with the experiment (see the mentioned left step in figure 1(*b*)).

The principal feature of the topographs (figures 2(*b*) and (*c*)) is the presence of three interference fringes, which are placed in the region of the wedge and marked as 1–3. Their number $m = 3$ was unchanged when reflections 113, −113, 1–13 and −1–13 were used. Similar contrast was observed in topographs recorded with 224 and 004 reflections, but the fringes number was $m = 4$.

The number of interference fringes can be explained within the framework of models [15, 16]. Using the formula $t_{\min} \approx (a/\delta a)d_{hkl}/\cos \varphi$ and taking $\delta a/a = 0.0069$ if $x = 0.09$, and $\delta a/a = 0.015$ if $x = 0.2$, one gets the next values of $t_{\min}$ for 113, 224 and 004 reflections: $t_{\min(113)} = 26.3$ and $t_{\min(224)} = t_{\min(004)} = 19.7$ nm for $x = 0.09$, and $t_{\min(113)} = 11.8$, $t_{\min(224)} = t_{\min(400)} = 8.87$ nm for $x = 0.2$. Correspondingly, the ratio of numbers of the visual fringes must be 4 : 4 : 3 for reflections 224, 004 and 113 in agreement with experimental results. If the number of the observed fringes is m, then the maximum thickness value of the crystal

layer $\mathbf{B}$ can be estimated as $mt_{\min} < t < (m + \frac{1}{2})t_{\min}$, since the number of observable fringes can be determined with an accuracy of $\frac{1}{2}$. The observed numbers m permit estimating the maximum separating layer thickness as 80–90 nm for the heterosystem (figure 2(*a*)) in agreement with technology data.

Rocking curves obtained using 004 reflection are plotted in figure 4 for the GeSi wedge region of the sample (figure 2(*a*)). Each subsequent curve was obtained by 0.25 mm displacement of the sample with respect to the incident beam along the thickness gradient. One can observe systematic change in the peak shape through the curves of this family. The rocking curve 1 has a broad flank on the side of small angles. The peak in curve 2 is almost symmetrical, it is similar to the peak of the bulk Si. Curve 3 has a broad flank on the side of large angles. The peak in curve 4 is broadened symmetrically. The subsequent curves are mirror images of the above curves. Another specific feature of these curves is the absence of Pendellösung maxima in curves 2 and 7 and their most conspicuous appearance in curve 4. A similar shape of peaks is observed in [3], where x-ray scattering from a quantum-well structure with varying well thickness of the separating InGaAs layer is simulated. According to conclusions [3], curves 2 and 7 correspond to the well thickness of $mN_{\min}d_{004}$ (the in-phase condition), and curve 4 corresponds to $(m+\frac{1}{2})N_{\min}d_{004}$ (the anti-phase condition). Here $d_{004} = a/4$ is the interplane spacing which is the same for the upper film and substrate.

Thus, the presented evolution of the rocking curves is associated with SiGe thickness variation in excess of $t_{\min}$. The dispersion of the maximum intensity values is within several percentages. As for densitometer track taken in the direction perpendicular to interference fringes 1–3 in the topographs (figures 2(*b*) and (*c*)), the difference between the maximum
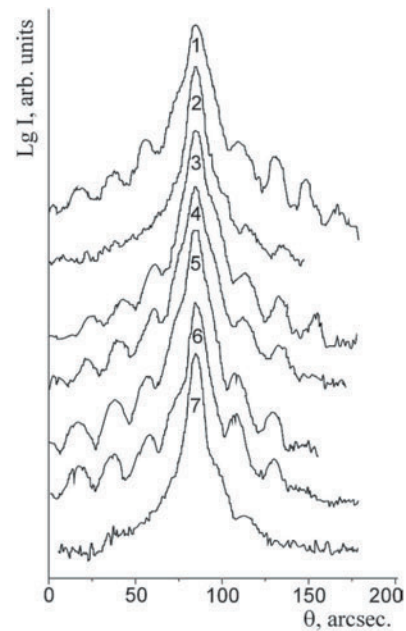
Figure 4. Family of experimental rocking curves registered for different thicknesses of $Ge_{0.09}Si_{0.91}$ layer. The in-phase condition takes place for curves 2 and 7, and the anti-phase one takes place for curve 4. Curves 2, 4 and 7 correspond to the lines A, E and B, accordingly, indicated in figure 3.

and minimum values is considerable. The contradictory is remedied by the assumption that the crystal angular position corresponding to peaks in the rocking curves 1–7 (figure 4) depends on the SiGe thickness. This assumption results from the comparison of the topographs presented in figures 2(b) and (c), which were obtained with different crystal angular positions. One can see displacement of interference fringes.

Numerical data concerning the mentioned angular peak position can be got from contrast analyses using the topograph (figure 3(a)). This topograph was recorded with 004 reflection using a convergent incident beam. The transition from one point to another along the direction **g** in the topograph corresponds to rotation of the crystal, which takes place when the rocking curve is registered. Thus, using a spherical monochromator gives possibility to register a lot of rocking curves within a single topograph.

Narrow periodical continuous Pendellösung fringes with a lowered intensity in parallel to the central wide intense strip are seen in the right part of the topograph (figure 3(a)). An estimated angle interval corresponding to the neighbouring fringes in the topograph is $w = 18$ arcsec in agreement with the angular distance between Pendellösung maxima in the rocking curve (see figure 4). This angular distance corresponds to the upper film thickness $t_{Si} = 1\,\mu$m. The mentioned fringes become discontinuous in the left part of the topograph (figure 3(a)), which corresponds to the wedge region of the GeSi separator. Here fringes transform into segments with inhomogeneous contrast along their length. The contrast vanishes if the lines A, B, C and D intersect the fringes. Therefore, one may conclude that along these lines the in-phase condition $t = mN_{min}d_{004}$ is met with $m = 1, 2, 3$ and 4 for the lines A, B, C and D, correspondingly.

Along the line E the anti-phase condition $t = (m + \frac{1}{2})N_{min}d_{004}$ is met with $m = 1$. It is also seen that the average direction of the segments in the left part of the topograph is not parallel to continuous fringes in the right part of the picture. These segments are shifted along the mentioned lines A, B, C and D. Thus, if the thickness of the intermediate layer increases from $t_1 = mt_{min}$ to $t_2 = (m + 1)t_{min}$, then the angular position of any Pendellösung maximum varies by w. This variation is in agreement with calculation results obtained using the semikinematical approximation [25]. According to [10] the intensity of the diffracted wave can be written for the in-phase conditions as

$$R(\Delta\theta) = R_p(\Delta\theta)\left[3 - 4\sin\left(\frac{\varphi_0}{2}\right)\sin\left(\frac{\varphi_0}{2} + \varphi_\alpha\right)\right],$$

where $\varphi_\alpha = 2\pi(\lambda\sin\theta_B)^{-1}[\chi_0 + \Delta\theta\sin2\theta_B]t$, $\varphi_0 = 2\pi(\lambda\sin\theta_B)^{-1}[\chi_0 + \Delta\theta\sin2\theta_B]t_{Si}$, $R_p(\Delta\theta)$ is the reflectivity profile of the perfect Si substrate and $\Delta\theta$ is the angular deviation from the kinematical Bragg angle. The calculation shows that for thickness change of t_{min} the variation of $\Delta\theta$ is equal to 19 arcsec in agreement with topography data of figure 3(a). The simulated image is shown in figure 3(b). It clearly demonstrates the discussed above contrast peculiarities of figure 3(a). Thus, the main observed topography features can be explained in the framework of semikinematical approach [10].

The obtained results give possibility to correct the data presented in figure 4. The crystal angular position, which corresponds to the peak in curve 7, will be considered as correct. Then the peak positions of curves 6, 5, 4 and 3 must be shifted at the values of 3.6, 7.2, 10.8 and 14.4 arcsec, correspondingly. The peak positions of curves 2 and 7, as well as those of curves 1 and 6, must coincide.

In the present investigation, the maximum value of peak variation equals w, which depends on the thickness of the upper film t_{Si}. It is likely that with t_{Si} change the angular amplitude of peak variation also changes. This question is under investigation. For the transmission geometry, the influence of t_{Si} value on the displacement of Moiré fringes was discussed in [20]. However, the presence of the intermediate layer was neglected.

4. Conclusion

For the three-layer $A/B/A$ heterosystem with perfect crystals, the intensity variations in topographs, which are associated with inhomogeneous thickness of the intermediate layer B, are investigated. In advancement of the model [16] it can be shown that inhomogeneous distortions in crystals A are not necessary for observation of these intensity variations. The displacement of interference fringes in topographs recorded by using a spherically bent monochromator gives possibility to reveal the dependence of the angular peak position of the rocking curve on the thickness of B. For 1 μm thick GeSi layer the maximum angular value of peak variation equals about 18 arcsec.

Acknowledgments

References

[1] Chu X and Tanner B K 1986 *Appl. Phys. Lett.* **49** 1773
[2] Ryan T W, Hatton P D, Bates S, Watt M, Sotomayor-Torres C, Claxton P A and Roberts J S 1987 *Semicond. Sci. Technol.* **2** 241
[3] Holloway H 1990 *J. Appl. Phys.* **67** 6229
[4] Chu X and Tanner B K 1987 *Semicond. Sci. Technol.* **2** 765
[5] Wie C R 1989 *J. Appl. Phys.* **65** 1036
[6] Jeong J, Schlesinger T E and Milnes A G 1988 *J. Cryst. Growth* **87** 265
[7] Tanner B K and Halliwell M A G 1988 *Semicond. Sci. Technol.* **3** 967
[8] Tanner B K 1993 *J. Phys. D: Appl. Phys.* **26** A151
[9] Krost A, Heinrichsdorff F, Bimberg D, Darhuber A and Bauer G 1996 *Appl. Phys. Lett.* **68** 785
[10] Milita S and Servidori M 1996 *J. Appl. Phys.* **79** 8278
[11] Simon D and Authier A 1968 *Acta Cryst.* A **24** 527
[12] Bonse U, Hart M and Schwuttke G H 1969 *Phys. Status Solidi* **33** 361
[13] Wieteska K 1981 *Phys. Status Solidi* a **68** 179
[14] Vasilenko A P, Kolesnikov A V, Nikitenko S G, Fedorov A A, Sokolov L V, Nikiforov A I and Trukhanov E M 2001 *Nucl. Instrum. Meth. Phys. Res.* A **470** 110
[15] Bonse U and Hart M 1969 *Phys. Status Solidi* **33** 351
[16] Ohler M, Härtwig J and Prieur E 1997 *Acta Cryst.* A **53** 199
[17] Ohler M, Prieur E and Hartwig J 1996 *J. Appl. Cryst.* **29** 568
[18] Ohler M, Köhler S and Härtwig J 1999 *Acta Cryst.* A **55** 423
[19] Polcarova M 1978 *Phys. Status Solidi* a **47** 179

[20] Ohler M and Härtwig J 1999 *Acta Cryst.* A **55** 413
[21] Yoshimura J 1991 *Phys. Status Solidi* a **125** 429
[22] Haroutyunyan V S 1996 *Crystallogr. Rep.* **41** 915
[23] Wieteska K and Wierzchowski W K 1995 *Phys. Status Solidi* a **147** 55
[24] Kolesnikov A V, Vasilenko A P, Trukhanov E M, Sokolov L V, Fedorov A A, Pchelyakov O P and Romanov S I 2000 *Appl. Surf. Sci.* **166** 82
[25] Kyutt R N, Petrashen P V and Sorokin L M 1980 *Phys. Status Solidi* a **60** 381